High-Pressure Sonoelectrochemistry in Aqueous Solution: Soft Cavitation under CO_2

Darío L. Goldfarb,[†] Horacio R. Corti,[†] Frank Marken,[‡] and Richard G. Compton*,[‡]

Physical and Theoretical Chemistry Laboratory, Oxford University, Oxford OX1 3QZ, United Kingdom, and Comisión Nacional de Energía Atómica, Unidad de Actividad Química, Av. del Libertador 8250 (1429), Buenos Aires, Argentina

Received: March 24, 1998; In Final Form: July 28, 1998

A novel high-pressure sonoelectrochemical cell has been developed in order to study the effect of pressure on cavitation and acoustic streaming in electrochemical processes. The reversible one electron reduction of a solution of $Ru(NH_3)_6^{3+}$ in aqueous 0.1 M KCl at a 25 μm diameter Pt microdisk electrode was studied under up to 60 bar pressure of argon and carbon dioxide and in the presence of ultrasound. The resulting cathodic current response was interpreted to be composed of a steady macroscopic streaming induced component and a transient spikelike component detected after the onset of the cavitation. The threshold for the cavitation process was strongly dependent on pressure and increased monotonically in the presence of argon. However, the threshold appeared at lower ultrasound power when pressurizing with carbon dioxide and even decreased at higher pressures (>40 bar) in the presence of CO_2. The analysis of the observed phenomena is possible in terms of the mechanical pressure, the surface tension, and the formation of a liquid CO_2 phase.

Introduction

The methodological overlap of ultrasonic irradiation and electrochemical techniques offers several major advantages over conventional electroanalytical techniques.[1] The activation and cleaning of electrode surfaces,[2] the removal of gas bubbles evolving at the electrode,[3] and improvements in mass transport to the electrode through acoustic streaming phenomena and cavitation[4] have been described. Beneficial effects of ultrasound on electroplating,[5,6] electrosynthesis,[7,8] and electropolymerization[9] and fundamental studies on the mechanisms by which ultrasound can modify electrochemical reactions have been reported.[10]

However, the appealing effects of ultrasound on mass transport and surface properties have hitherto always been limited to atmospheric pressure conditions. The combination of high-pressure and ultrasound assisted electrochemistry explored in the present study is intended to contribute to the development of processes under nonclassical conditions and/or in new reaction media,[11] with potential applications in technological problems involving high-pressure and supercritical electrochemistry.

Experimental Section

Reagents. The electrochemical experiments were performed using high-purity water of resistivity not less than 18 MΩ cm (Elgastat, High Wycombe, Bucks), hexaammineruthenium(III) chloride (98%, Aldrich), potassium chloride (99+%, Aldrich), Pureshield argon (BOC Gases), and carbon dioxide (99+%, The Distillers Co.). Solutions were purged with carbon dioxide or argon at 1 bar ambient pressure before being transferred into the sonoelectrochemical cell in order to presaturate them with the selected gas.

Cell Design. In Figure 1 the geometry of the high-pressure sonoelectrochemical cell is shown. It consists of three main blocks (A−C) and is entirely constructed with materials inert to most organic solvents and acidic or basic media.

Block A consists of a titanium block, shaped to contain the working electrode (6), a 25 μm diameter Pt wire (Goodfellow) sealed in a glass tube (6 mm o.d., 1 mm i.d.). A silver wire welded to the Pt microwire acts as an external contact. The high-pressure sealing for the microelectrode is achieved through PTFE gaskets (5) compressed by titanium washers against the glass tube and the walls of the Ti block. A brass nut (14) exerts the necessary pressure on the Ti washers to keep the sealing tightly closed. A brass counternut (15) prevents the microelectrode tubing from being ejected from the cell due to the high applied pressure.

Block B includes a titanium body that contains a couple of sapphire windows (3), each one glued (UHU) to a titanium counternut. The windows compress a PTFE washer (4) against the titanium body in order to achieve the desired sealing. In this way visual observations of the cell interior are possible under high pressure.

Three HPLC inlets (only one shown in Figure 1) for $^1/_{16}$ in. tubing (7) are used for the Ag quasi-reference electrode, the gas inlet, and a temperature sensor. The quasi-reference electrode was a 1 mm diameter silver wire (Goodfellow) coiled around the glass tube of the microdisk working electrode. The high-pressure sealing was achieved with a PTFE cone and a $^1/_{16}$ in. LiteTouch PEEK nut (Upchurch Scientific). PEEK tubing of $^1/_{16}$ in. o.d. and 0.01 in. i.d. (Upchurch) was used to deliver the gases to the cell through one of the inlets. Blocks A and B are tightly held in place through five tensile bolts compressing a 0.5 mm gold O-ring so as to provide an effective pressure sealing.

Block C contains the ultrasound source. A VC100 ultrasound generator (Sonics and Materials) converts 50/60 Hz mains voltage to a 20 kHz signal which is transmitted to the piezoelectric transducer. The resonating horn probe (2) is of 14 cm overall length and ends in a 3 mm diameter tip immersed in the aqueous solution. A PTFE cone (11) compressing the

[†] Unidad de Actividad Química.
[‡] Oxford University.

10.1021/jp9815964 CCC: $15.00
Published on Web 10/09/1998

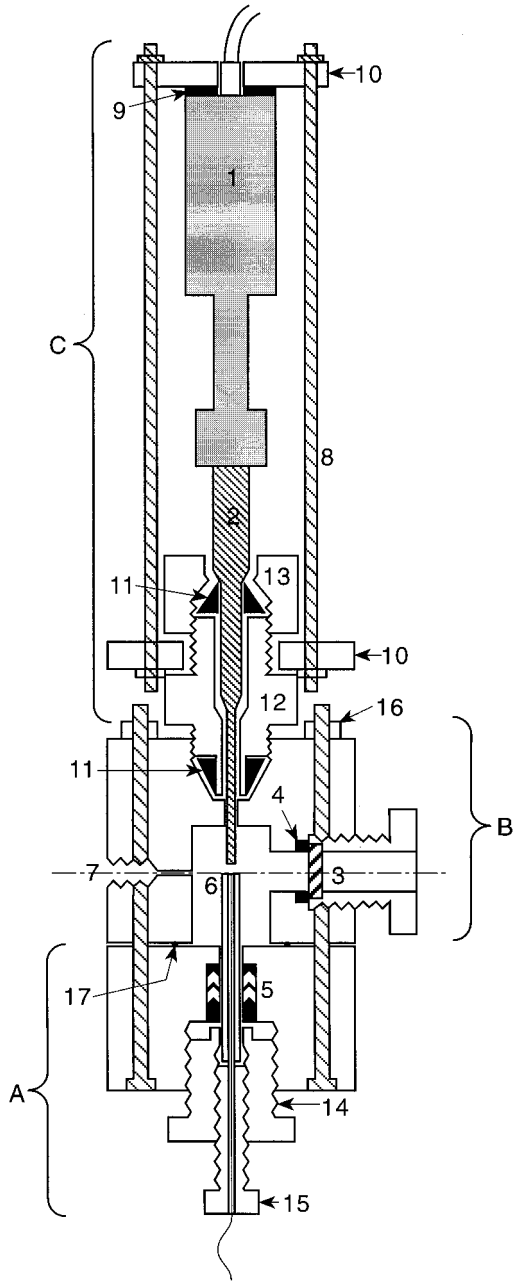

Figure 1. Schematic drawing (1:2 scale) of the high-pressure sonoelectrochemical cell: (1) Ultrasound converter; (2) tip horn; (3) sapphire window; (4) PTFE O-ring; (5) PTFE gaskets and Ti washers; (6) 25 μm Pt microelectrode; (7) inlet; (8) brass threaded bars; (9) PTFE washer; (10) aluminum disk; (11) $^1/_4$ in. PTFE cone; (12) titanium double nut; (13) titanium counternut; (14) brass nut; (15) brass counternut; (16) tensile bolt; (17) gold O-ring.

$^1/_4$ in. diameter body of the probe proved to be a effective high-pressure seal for the horn. Another PTFE cone (11) was used to hold the probe in a face-on position toward the microdisk working electrode situated at a distance of ca. 2 mm from the horn.

Three threaded bars (8) compressing two aluminum disks (10) were used to position the horn probe within the cell. A PTFE washer (9) separated the metallic case of the converter from the aluminum disk to achieve electrical insulation of the cell body from the transducer. The body of the electrochemical cell was used as the auxiliary electrode.

The volume of the high-pressure electrochemical cell was ca. 15 cm^3. The cell was tested up to 100 bar pressure without any noticeable leak over a period of several hours. To quantify

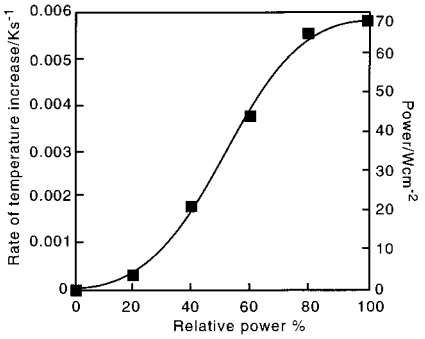

Figure 2. Calibration of the ultrasonic signal output by relating the temperature rise after a short period of sonication and thermal equilibration of the cell (given in temperature rise (K) per sonication period (s)) and the approximate intensity (W cm^{-2}), calculated with a heat capacity estimate for the system, as a function of the nominal power.

the amount of power delivered from the ultrasonic source into the system, the rise in temperature (ΔT) of the cell and 11 cm^3 of water after a short period of ultrasonic irradiation was correlated with the intensity of the source. At ambient pressure a linear relation between ΔT and the ultrasound intensity was observed between 20 and 80% of the maximum power available (see Figure 2). From the measured temperature rise after a short sonication period the approximate intensity of the horn probe could be estimated by assuming that the cell body (ca. 330 cm^3) and the water (ca. 11 cm^3) converge toward thermal equilibrium. The results (shown in Figure 2) are probably lower limits and consistent with those described for similar horn probes immersed in an aqueous solution.[12] The effect of applied pressure on the ultrasound intensity emitted from the horn probe appeared not to be significant on the basis of the data obtained with argon as the pressurizing gas (vide infra). However, this effect may not always be assumed to remain small, and depending on the horn probe diameter and the range of pressures employed, the calibration procedure has to consider pressure effects.

Instrumentation. Pressure was monitored with a 0−350 bar EPX pressure transducer (Entran Devices) mounted on a stainless steel support. The pressure accuracy was ±0.5 bar for all measurements. The temperature inside the sonoelectrochemical cell was registered with a CAL 3200 temperature controller (CAL Controls) and a K-type thermocouple inserted in 1.5 mm stainless steel tubing. The thermocouple was positioned 5 mm away from the horn tip, so that temperature changes due to mechanical energy that dissipated into heat could be recorded. A $^1/_{16}$ in. PEEK ferrule and LiteTouch nut (Upchurch) proved to be an effective pressure seal for the thermocouple.

Electrochemical data were recorded using a bipotentiostat (Oxford Electrodes), configured in such a way that the horn potential (second working electrode) was set to 0 V versus the Ag pseudo-reference electrode to avoid undetected currents flowing to or from the horn tip. The current follower employed allowed data acquisition of nondistorted signals down to a 10 μs time scale. The current−voltage output was recorded either with a PL3 Plotter (Lloyd Instruments) for voltammograms or with a Gould 1600 Oscilloscope (10 MHz, Gould Electronics) for time-resolved measurements.

Results and Discussion

To study the effect of pressurizing the sonoelectrochemical cell with argon and carbon dioxide, an inert redox probe with a well-defined electrochemical response at a Pt electrode in

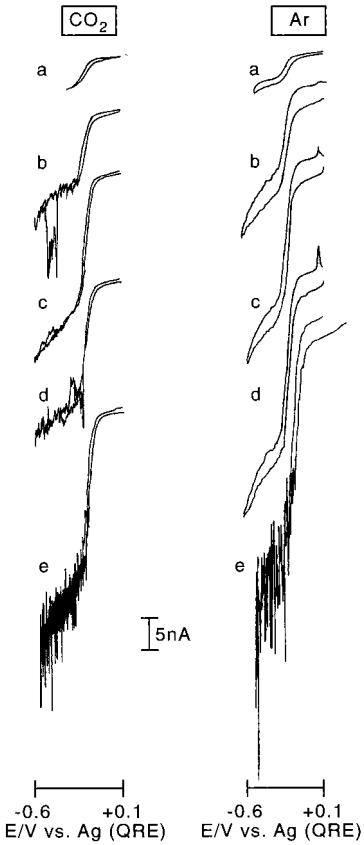

Figure 3. Cyclic voltammograms for the reduction of 1 mM $Ru(NH_3)_6Cl_3$ in 0.1 M KCl aqueous solution obtained at a 25 μm diameter Pt microdisk electrode at 20 °C. Scan rate, 50 mV/s. Conditions: CO_2, 8.3 bar, (a) silent, (b) 1%, (c) 10%, (d) 20%, and (e) 30% relative ultrasound power; Ar, 8.9 bar, (a) silent, (b) 10%, (c) 30%, (d) 50%, and (e) 60% relative ultrasound power.

aqueous media is required and the reversible $Ru(NH_3)_6^{3+/2+}$ redox couple was employed.[13]

$$Ru(NH_3)_6^{3+} + e^- \rightleftarrows Ru(NH_3)_6^{2+} \qquad (1)$$

This "electrochemical probe" can be used to reliably detect ultrasound induced mass transport phenomena at the electrode|solution interface and the threshold at which bubble growth, expansion, and collapse starts to occur.[4] Intense ultrasound is known to cause a multitude of complex phenomena such as turbulent flow,[14] bubble oscillation, and cavitation,[15,16] leading to the generation of microjets and shock waves, which are partly responsible for the massive increase in the rate of mass transport observed in electrochemical experiments.

Cyclic voltammograms recorded in the presence of ultrasound differ considerably from those recorded under silent conditions. In Figure 3 cyclic voltammograms for the reduction of $Ru(NH_3)_6^{3+}$ in aqueous 0.1 M KCl at a 25 μm diameter Pt disk electrode and at ca. 8 bar under silent conditions are shown. Well-defined sigmoidally shaped near-steady-state responses were detected. The limiting current for these responses was in close agreement (within 5%) with those predicted for a diffusion coefficient[13] $D_{Ru} = 9.1 \times 10^{-10}$ m^2 s^{-1}. Due to the relatively high scan rate of 50 mV s^{-1} which has been used in order to minimize possible thermal effects, this deviation from the ideal steady-state limiting current may be accepted. A change in pressure of up to 60 bar did not alter the diffusion-limited current for the reduction process under silent conditions and is not expected to alter the diffusion coefficient significantly.[17]

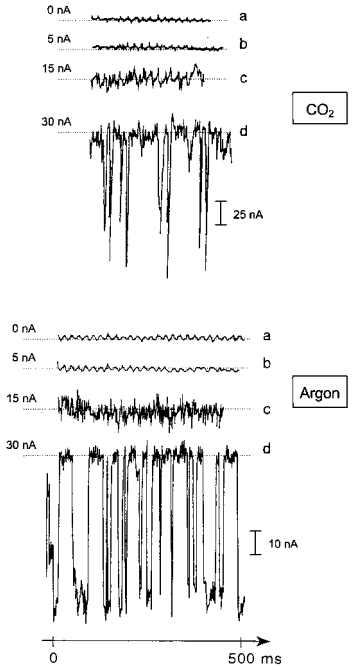

Figure 4. Time dependent response for the reduction of 1 mM $Ru(NH_3)_6Cl_3$ in 0.1 M KCl aqueous solution at a 25 μm diameter Pt microdisk electrode. Conditions: CO_2, 43 bar, (a) E (vs pseudo-Ag) = +200 mV, silent; (b) −600 mV, silent; (c) −600 mV, 20% relative power; (d) −600 mV, 40% relative power; Ar, 4.1 bar, (a) E (vs pseudo-Ag) = +200 mV, silent, (b) −600 mV, silent, (c) −600 mV, 30% relative power, (d) −600 mV, 40% relative power. Current traces are not on a common scale and are referenced by a dotted line.

In the presence of ultrasound, the mean transport limited current is remarkably increased as compared to the silent case (Figure 3). After switching on the ultrasound power, two different types of behavior were observed. First, at a given pressure and at low ultrasonic power, no cavitation occurred on the basis of the absence of current fluctuation as well as on visual observation through the sapphire window of the cell. Under these conditions, only convection possibly due to macroscopic acoustic streaming[18] was revealed through an increased limiting current compared to silent conditions. The flow rate responsible for the observed increase of current which may be estimated on the basis of a diffusion layer thickness of ca. 10 μm and on the equation for the "wall tube" geometry[18] is found on the order of 10 cm s^{-1}. Acoustic streaming is an effect induced by sound absorption and strongly dependent on the horn and cell geometry, with smaller horn diameters causing more facile streaming. Second, after a pressure dependent threshold in ultrasound power, the onset of cavitation at the electrode|solution interface is observed as a jump in the limiting current and additional current spikes are detected (Figure 3e).

However, the Faradaic current response described by the cyclic voltammograms is a time-averaged value of a rapidly fluctuating current. The transient current components are more clearly resolved when a fixed potential of −0.6 V vs Ag-pseudoreference is applied and the time-dependent signal is recorded with an oscilloscope (Figure 4). The current traces shown are recorded in the presence of carbon dioxide (41.3 bar) and argon (4.1 bar). The presence of cavitation events at higher ultrasound power is obvious, and a considerable difference in the magnitude of the cavitation induced current spikes can be seen. The magnitude of these current spikes appears to be about twice that of the steady background current in the presence of carbon dioxide at 41.3 bar pressure and in the presence of argon at 4.1 bar pressure.

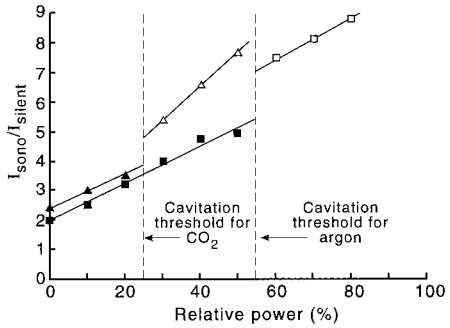

Figure 5. Effect of the onset of cavitation on the I_{sono}/I_{silent} ratio for the reduction of 1 mM $Ru(NH_3)_6Cl_3$ in 0.1 M KCl aqueous solution at 20 °C. Conditions: CO_2, (8.3 bar, (▲) no cavitation, (△) cavitation observed; Ar, 8.9 bar, (■) no cavitation, (□) cavitation observed.

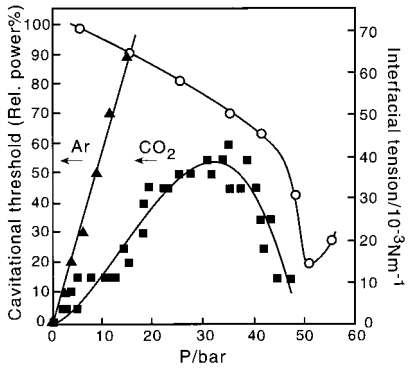

Figure 6. Plot of the variation of the cavitational threshold for a 1 mM $Ru(NH_3)_6Cl_3$ in 0.1 M KCl aqueous solution at 20 °C as a function of pressure for argon (▲) and carbon dioxide (■). Also shown is the interfacial tension for the system CO_2-H_2O (○) at 20 °C as a function of pressure, after interpolation of data from ref 26.

The onset of cavitation at the electrode|solution interface was detected reproducibly at a threshold of ultrasonic power which changed with the applied pressure and the type of gas present. Although a consistent picture emerged from the electrochemical detection of cavitation events and from noise and visual observations, it has to be stressed that the threshold for cavitation at a solid|solution interface may be significantly lower compared to the threshold for cavitation in bulk solution. In a solution phase impurities such as dust particles are commonly believed to be the sites where nucleation of cavitation bubbles occurs. However, at a solid|solution interface the flow of the liquid creates an additional tension which, under extreme conditions, can be sufficient to cause cavitation even in the absence of sound.

In Figure 5 typical traces for the change in average limiting current with applied sound intensity for 8.3 bar CO_2 and for 8.9 bar Ar are shown. In general, an increase in current is detected and a jump in the limiting current and the onset of current fluctuations indicate the threshold for cavitation at the interface. With these criteria, the cavitation threshold was defined as the relative power halfway between the highest power at which cavitation was not observed and the lower power needed to produce cavitation.

The effect of pressurizing the sonoelectrochemical cell either with argon or carbon dioxide on the threshold for cavitation is shown in Figure 6. A very dramatic difference even at low applied pressures can be seen. In the presence of argon a nearly linear increase suggests a strong influence of the pressure and at a relatively mild 30 bar level cavitation could not be induced anymore with the available ultrasound power. The low solubility of argon in water at room temperature[19] makes this pressurizing fluid very similar to a "mechanical pump". The effect of applying an argon pressure affects the cavitation threshold mainly in terms of pressure variation. When the pressure is increased, higher ultrasound intensities are needed to make the cavitation process appear to be in qualitative agreement with proposed models for cavitation.[20]

A simple approach for describing the onset of the explosive growth of a bubble, which may be regarded as the initial phase before cavitational collapse can occur, is the so-called Blake threshold pressure (P_B). It assumes that only the external pressure (P_o), the vapor pressure (P_v), the surface tension (σ), and the equilibrium radius of the bubble (R_o) determine the necessary negative pressure in the liquid (P_L) to produce an explosive expansion of a bubble:[21]

$$P_L = P_o - P_B = P_v - \frac{4}{3}\sigma\left[2\sigma/3R_o^3\left(P_o + 2\frac{\sigma}{R_o} - P_v\right)\right]^{1/2} \quad (2)$$

To describe such behavior fully, the inertial and viscous effects of the liquid have to be included. The Blake model ignores these, so restricting its application to the limit of very small bubbles. In these, the pressure induced by the surface tension $P_\sigma = 2\sigma/R_o$ tends to very large values, thereby dominating the other effects. Thus

$$P_B \approx P_o + 0.77\frac{\sigma}{R_o} \quad (3)$$

Therefore an increase of the cavitation threshold with applied pressure is expected. However, as will be shown for the case of carbon dioxide, this simple rule may be violated.

Being considerably more soluble, carbon dioxide exhibits a quite different behavior compared to argon. In Figure 6 it can be seen that although an initial rise in the cavitation threshold with pressure occurs, it is substantially less pronounced. This effect is believed to be related to the change in surface tension of the aqueous phase (see eq 3) which is more pronounced in the presence of CO_2. Further, at an applied pressure of ca. 40 bar the cavitation threshold suddenly decreases with increasing pressure. The purely mechanical pressure effect observed for argon appears to be opposed by the fact that the high solubility[22] of CO_2 provides a more effective medium for cavitation. Thus, at a given pressure, the onset of cavitation for carbon dioxide appears always at lower ultrasound power compared to argon. For comparison, the Henry's law constant ratio for argon and carbon dioxide [$k_H°(Ar)/(k_H°(CO_2)$] is about 15 at 20 °C.[19,22] For CO_2, the hydrolysis process to produce H_2CO_3, HCO_3^-, and CO_3^{2-} species may be neglected due to the small value of the hydrolysis constants,[23,24] indicating that the extent of this hydration process under the conditions considered would be negligible. Therefore carbon dioxide dissolved in water appears to act as an efficient promoter for cavitation events which are detected at the electrode|solution interface.

In addition to this observation, as another feature at high pressure of CO_2 above 40 bar, a decrease in the cavitation threshold was noticed. As the pressure is increased for a system characterized by a point below line E in the phase diagram[25] (see Figure 7), there will be two phases with a composition given by the line B (aqueous phase) and the line C (gaseous phase). At a pressure of about 50−55 bar line E indicates the formation of a new liquid phase, a carbon dioxide rich liquid, in what is now a three phase system. The pressure fluctuation

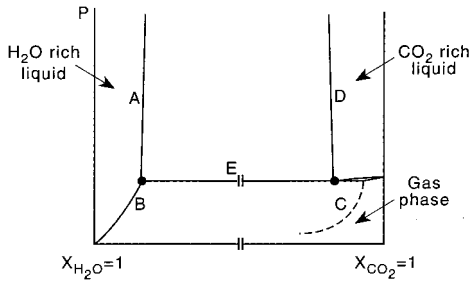

Figure 7. Schematic phase diagram for the system CO_2-H_2O below the critical temperature of carbon dioxide, adapted from data in ref 25.

TABLE 1: Interfacial Tension Data for the System CO_2-H_2O at 20 °C Interpolated from Data at 5, 10, 15, and 25 °C Taken from Ref 26

P (bar)	γ (mN/m)	P (bar)	γ (mN/m)
5.0	70.1	41.4	45.4
15.0	64.3	48.3	30.8
25.0	57.7	51.0	14.5
35.0	50.1	55.2	20.1

due to the pressure amplitude of the sound wave may be estimated from the expression[20]

$$I = P_A^2/\rho c \qquad (4)$$

In this equation P_A denotes the pressure amplitude, ρ the density, and c the velocity of sound in water. For a relative power of 100% or a corresponding intensity of ca. 69 W cm^{-2} (see Figure 2), the pressure amplitude in the vicinity of the horn probe may be estimated on the order of 10 bar. Therefore the transition from a two phase system to a three phase system may occur transiently under sonication and at a static pressure below that predicted from the phase diagram. As the pressure drops in the sound duty cycle and the total pressure becomes less than that required for the formation of the carbon dioxide rich liquid, the resulting local oversaturation with CO_2 could result in a facile nucleation of a new cavitation bubble.

Among the many parameters that could contribute to the decrease in the cavitation threshold, the interfacial tension variation with pressure appears to be important. Equation 3 predicts a reduction in the cavitation threshold if the surface tension is reduced. Interfacial tension data for the system water$-CO_2$ at 5, 10, 15, and 25 °C have been published[26] and a linear interpolation to 20 °C was used in order to adapt the data to the case discussed here (see Table 1). A pronounced decrease in surface tension is observed as conditions for the formation of the liquid CO_2 phase are approached, and a minimum in surface tension marks the conditions where the new phase finally appears. This drop in surface tension is not limited to the conditions in the vicinity of the mixture critical point but spans a wide region, down to 40 bar (see upper line in Figure 6). The surface tension effect possibly dominates the other effects mentioned before (solubility and mechanical pressure) in this region of the phase diagram.

The violence or force of cavitation events is known to change with the applied pressure, e.g. from erosion in marine environments.[21b] On the other hand the nature of the gas dissolved in the aqueous phase also has a strong effect on the characteristics of the cavitation process.[27,28] The "soft" nature of cavitation in the presence of carbon dioxide has been described and linked to solubility, thermal conductivity, and the polytropic ratio[21b] for applied ultrasound at ambient pressure.[27,28] The effect of surface tension and the proposed transient formation of a new phase at elevated pressure appear to further add to these effects. On the other hand the magnitude of the induced current spike in time-resolved amperometric traces appears not to be strongly linked to the violence of the cavitation process, and current enhancement remains significant.

Conclusions

High-pressure sonoelectrochemical experiments up to 100 bar static pressure and employing high-intensity ultrasound emitted from an ultrasonic horn probe are possible in a novel versatile cell arrangement. The effect of pressure on an electrochemical process in an aqueous medium and in the presence of ultrasound has been shown to be strongly dependent on the type of pressurizing gas. In the presence of carbon dioxide the threshold for cavitation becomes rather low at pressures near the region of phase formation, and a corresponding increase in the average limiting current may be achieved at relatively low ultrasound intensity.

A correlation between the ultrasound power needed to produce cavitation at the electrode|solution interface and the interfacial tension of the solution phase has been detected. Due to the current enhancement detected even in the presence of "soft" cavitation, other systems such as liquids near the critical point could be very suitable solvents for efficient sonoelectrochemical processes, even at high applied pressures.

Acknowledgment. D.L.G. acknowledges a fellowship from British Council−Fundación Antorchas, and F.M. thanks the Royal Society for a University Research Fellowship and New College (Oxford) for a stipendiary lectureship.

References and Notes

(1) For a review, see, for example: Walton, D. J.; Phull, S. S, *Adv. Sonochem.* **1996**, *4*, 205.

(2) Compton, R. G.; Eklund, J. C.; Page, S. D.; Sanders, G. H. W.; Booth, J. *J. Phys. Chem.* **1994**, *98*, 12410.

(3) Cataldo, F. *J. Electroanal. Chem.* **1992**, *332*, 325.

(4) (a) Klima, J.; Bernard, C.; Degrand, C. *J. Electroanal. Chem.* **1995**, *399*, 147. (b) Birkin, P. R.; Silva-Martinez, S. *J. Electroanal. Chem.* **1996**, *416*, 127. (c) Perusich, S. A.; Alkire, R. C. *J. Electrochem. Soc.* **1991**, *138*, 708.

(5) Namgoong, E.; Chen, J. S. *Thin Solid Films* **1984**, *120*, 153.

(6) Walker, R. *Chem. Br.* **1990**, *26*, 251.

(7) See for example: (a) Mason, T. J.; Lorimer, J. P.; Walton, D. J. *Ultrasonics* **1990**, *28*, 333. (b) Atobe, A.; Matsuda, K.; Nonaka, T. *Denki Kagaku*, **1994**, *62*, 1298. (c) Durant, A.; Francois, H.; Reisse, J.; Kirsch-DeMesmaeker, A. *Electrochim. Acta* **1996**, *41*, 277.

(8) Marken, F.; Compton, R. G.; Davies, S. G.; Bull, S. D.; Thiemann, T.; Sa e Melo, M. L.; Neves, A. C.; Castillo, J.; Jung, C. G.; Fontana, A. *J. Chem. Soc., Perkin Trans. 2* **1997**, 2055, and references cited therein.

(9) Osawa, S.; Ito, M.; Tanaka, K.; Kuwano, *J. Synth. Met.* **1987**, *18*, 145.

(10) Compton, R. G.; Eklund, J. C.; Marken, F. *Electroanalysis* **1997**, *9*, 507.

(11) See for example: Van Eldik, R., Hubbard, C. D., Eds. *Chemistry under Extreme or Non-Classical Conditions*; Wiley: New York, 1997.

(12) Hill, H. A. O.; Nakagawa, Y.; Marken, F.; Compton, R. G. *J. Phys. Chem.* **1996**, *100*, 17395.

(13) Marken, F.; Eklund, J. C.; Compton, R. G. *J. Electroanal. Chem.* **1995**, *395*, 335.

(14) Lighthill, J. *Waves in Fluids*; Cambridge University Press: Cambridge, U.K., 1978.

(15) Suslick, K. S. *Science* **1990**, *247*, 1439.

(16) Henglein, A. *Ultrasonics* **1987**, *25*, 6.

(17) Golas, J.; Drickamer, H. G.; Faulkner, L. R. *J. Phys. Chem.* **1991**, *95*, 10191.

(18) Marken, F.; Akkermans, R. P.; Compton, R. G. *J. Electroanal. Chem.* **1996**, *415*, 55.

(19) Potter, R. W.; Clynne, M. A. *J. Solution Chem.* **1978**, *7*, 837.

(20) Mason, T. J., Ed. *Sonochemistry: The Uses of Ultrasound in Chemistry*; Royal Society of Chemistry: Cambridge, U.K., 1990.
(21) (a) Blake, F. G. *Technical Memos No. 9 and No. 12*. Acoustics Research Laboratory, Harvard Unversity: Cambridge, MA, 1949. (b) Leigthon, T. J. *The Acoustic Bubble*; Academic Press: London, 1994.
(22) Vilcu, R.; Gainar, I. *Rev. Roum. Chim*. **1967**, *12*, 181.
(23) Wissburg, K. F.; Frenc, D. M.; Patersson, A. *J. Phys. Chem*. **1954**, *58*, 693.
(24) Ellis, A. J. *J. Chem. Soc. (London)* **1959**, 1765.
(25) King, M. B.; Mubarak, A.; Kim, J. D.; Bott T. R. *J. Supercrit. Fluids* **1992**, *5*, 296.
(26) Chun, B. S.; Wilkinson, G. T. *Ind. Eng. Chem. Res*. **1995**, *34*, 4371.
(27) (a) Leeman, S.; Vaughan, P. W. In *Current Trends in Sonochemistry*; Price, G. J., Ed., The Royal Society of Chemistry: Cambridge, U.K., 1992; p 30. (b) Suslick, K. S. *Ultrasound, Its Chemical, Physical, and Biological Effects*; VCH: Weinheim, Germany, 1988.
(28) Henglein, A.; GutiÉrrez, M. *J. Phys. Chem*. **1988**, *92*, 3705, and references cited therein.